NJC

Accepted Manuscript

This is an *Accepted Manuscript*, which has been through the Royal Society of Chemistry peer review process and has been accepted for publication.

Accepted Manuscripts are published online shortly after acceptance, before technical editing, formatting and proof reading. Using this free service, authors can make their results available to the community, in citable form, before we publish the edited article. We will replace this *Accepted Manuscript* with the edited and formatted *Advance Article* as soon as it is available.

You can find more information about *Accepted Manuscripts* in the Information for Authors.

Please note that technical editing may introduce minor changes to the text and/or graphics, which may alter content. The journal's standard Terms & Conditions and the Ethical guidelines still apply. In no event shall the Royal Society of Chemistry be held responsible for any errors or omissions in this *Accepted Manuscript* or any consequences arising from the use of any information it contains.

ROYAL SOCIETY OF CHEMISTRY

www.rsc.org/njc

Journal Name

ARTICLE

Highly flexible silica aerogel derived from methyltriethoxysilane and polydimethylsiloxane†

Received 00th January 20xx,
Accepted 00th January 20xx

DOI: 10.1039/x0xx00000x

www.rsc.org/

Liang Zhong,[a] Xiaohong Chen,*[a] Huaihe Song,[a] Kang Guo[a] and Zijun Hu*[b]

Highly flexible silica aerogels were synthesized using methyltriethoxysilane (MTES) and polydimethylsiloxane (PDMS) as co-precursors via a two-step acid-base sol-gel method followed by ambient pressure drying. The effects of volume ratio of PDMS to MTES (S) on the flexibility were investigated in detail. It was found that, with the increase of S from 5% to 8.75%, both the Young's modulus and density of obtained aerogels decrease from 0.136 to 0.030 MPa and 0.098 to 0.064 g·cm^{-3}, respectively. Aerogel produced at S of 8.75% shows excellent compressional and recoverable properties. Its maximal recoverable compressive strain is 70%. The unrecovered strains calculated immediately and 12 h after the compression to 60% strain for twenty times are 10.9 % and 3.1 %, respectively. The excellent flexibility performance of silica aerogel derived from MTES-PDMS makes it a promising silica aerogel material for special applications.

1. Introduction

The inherent disadvantages of traditional aerogels, such as high fragility and moisture sensitivity, severely restrict their applications.[1-4] Therefore, with the purpose of expanding the application range of aerogels, more flexible and/or hydrophobic aerogels are needed. In principle, flexibility and/or hydrophobicity can be introduced by the incorporation of organic parts into the inorganic networks. [5, 6] A range of silica aerogels with flexibility has been produced by introducing reactive functional groups onto the surfaces of the silica gel by coreacting functionalized trialkoxysilanes with conventional silane precursors such as tetramethoxysilane (TMOS) or tetraethoxysilane (TEOS).[7, 8] Nguyen had demonstrated that replacing a large fraction of tetramethoxysilane (TMOS) or tetraethoxysilane (TEOS), with bis(trimethoxysilyl)hexane (BTMSH) imparts flexibility to the TMOS or TEOS based silica aerogels reinforced with di-isocyanate[9], epoxy[10], or styrene[11]. Some of the more rigid Si-O-Si bones were replaced by the flexible hexyl bridging group of BTMSH. The resulting aerogels could recovery almost completely after compression of samples to 25% strain. In the same way, Guo et al.[12] combined a bridged silsesquioxane (triethoxysilyl)propyl]disulfide (BTSPD) with TMOS and vinyltrimethoxysilane (VTMS) to improve the flexibility and elastic recovery of silica aerogel. In addition, Randall et al.[13] had investigated the alkyl-linked silane, such as bis(triethoxysilyl)-ethane (BTESE), BTMSH and bis(triethoxysilyl)octane (BTESO), as well as dimethyldiethoxysilane (DMDES) as ways of altering the silica backbones for tailoring of mechanical properties. However, the use of relatively expensive bridged polysilsesquioxanes which are not widely available and the poor thermal stability of these polymer reinforced silica aerogels limit their widespread application.[14, 15]

Recently, silica aerogels with more flexibility have been fabricated through using trifunctional organosilane $R'_xSi(OR)_{4-x}$ ($1 \le X \le 3$, R'=methyl, or ethyl) as the sole or one of the precursors.[16] The organic group (R') can minimizes the inter-chain cohesion between silica polymer chains, which provides higher flexibility to products. For example, Rao had prepared flexible silica aerogels with compressibility as high as ~60% of the original length and Young's modulus as low as 1.094×10^4 N·m^{-2} by using organoalkoxysilanes as precursors, such as methyltrimethoxysilane (MTMS) [17]and memthyltriethoxysilane (MTES)[18, 19]. In addition, including propyl groups in the underlying silica skeleton of MTMS derived aerogel can also improve the flexibility of these MTMS-based silica aerogel, which can be compressed to 70% of their original height. [20]

Although these recent advancements lead to improved flexible properties of silica aerogels, the costly and hazardous process of supercritical drying (SCD), needing a special condition, such as high pressure and high temperature, limit their wide utility. [21, 22] In additional, choosing the cheaper non-alkoxide as precursors is an effective way to reduce the cost of aerogels.[23, 24] Nevertheless, the non-alkoxides precursors are more difficult to prepared aerogel with high flexibility due to the

[a] State Key Laboratory of Chemical Resource Engineering, Beijing Key Laboratory of Electrochemical Process and Technology for Materials, Beijing University of Chemical Technology, Beijing, 100029, P. R. China.
[b] National Key Laboratory of Advanced Functional Composite Materials, Aerospace Research Institute of Materials & Processing Technology, Beijing 100076, P. R. China.
*[a] Corresponding author. Fax/Tel.: +86-010-64434916; E-mail address: chenxh@mail.buct.edu.cn.
*[b] Corresponding author. Fax/Tel.:+86-010-68755517; E-mail address: huzijun@hotmail.com.
† Electronic Supplementary Information (ESI) available: The first 5 times of the 20 consecutive compression to 60% strain for aerogel S_5 (Movie M1). See DOI: 10.1039/b000000x/

complex modified treatment. Ambient pressure drying is a safer, cheaper and more practical method to make silica aerogels interesting for widespread commercial applications.[25-28] However, only a few reports on monolithic flexible trifunctional organosilane-derived silica aerogels via ambient pressure drying have been published. Kanamori et al.[29] reported the preparation of "marshmallow-like" aerogels from a mixture of MTMS and dimethyldimethoxysilane (DMDMS) by ambient pressure drying. However, these productions required surfactants and multiple solvent exchanges. Bhagat et al.[30] had prepared monolithic MTMS-based aerogel via ambient pressure drying whereas they did not have a detailed discussion on the flexibility performance. Aravind et al.[31]had synthesized the MTES-based aerogels by ambient pressure drying. However, the alcogels still needed to be aged in different concentrations of silane precursor solutions before drying. The Young's modulus and shrinkage were not mentioned.

Herein, we present a two-step acid-base sol-gel process for preparation of highly flexible, low-density and high hydrophobic aerogels using trialkoxysilane (MTES) and polydimethylsiloxane (PDMS) as co-precursor via ambient pressure drying. Disilanol-terminated polydimetylsiloxane (PDMS) is one of the excellent candidates for introducing the organic groups into the underlying silica structures to further improve the flexibility and elastic recovery of silica based aerogels because of its unique structure: the numerous organic methyl of PDMS, the similarity of its backbone structure (-Si-O) to the gel matrix of trialkoxysilane and the well elastic recovery via coiling/uncoiling of the PDMS chain. Besides, the more important fact is that the co-polycondesation between the terminal silanol groups of PDMS and the hydrolyzed MTES oligomer can occur under basic condition.[32] The adjacent silica secondary particulates are connected by the PDMS chain. In this paper, the effects of the amount of PDMS inclusion on the microstructure, textural and mechanical properties of the PDMS modified aerogels were examined. This synthesis is quite simple and practical for highly flexible silica aerogels, which is useful for applications that require flexibility.

2. Experimental section

2.1. Synthesis of MTES-PDMS based aerogels

All reagents were purchased from Sinopharm Chemical Reagent Beijing Co., Ltd (Beijing, China). Methyltriethoxysilane (MTES), polydimethylsiloxane (PDMS), methanol and ethanol were used as recevied. NH_4OH (25.0%~28% w/w) and oxalic acid ($C_2H_4O_2$) were used after beeing diluted to a certain concentration.

Silica alcogels were prepared via the hydrolysis and condensation of the precursor, aging, and subsequent drying, which is similar to the procedures described by Tillotson and Hrubesh.[33] In a typical run, for the molar ratio of MTES: MeOH: $C_2H_4O_2$ (0.001M):NH_4OH (10 M) at 1:27:4:4, 4 mL MTES was mixed with 22.4 mL MeOH and was then added $C_2H_4O_2$ (0.001M $C_2H_4O_2/H_2O$ solution) as the acidic catalyst. The resulting mixture was stirred for 0.5 h. After a 24 h interval, the disilanol-terminated polydimethylsiloxane (M_n=1085, tested) and NH_4OH (10 M NH_4OH/H_2O solution) were successively added to the solution drop by drop and stirred for another 0.5 h. Then, the obtained alcosols were transferred into ampoule tubing (25 mL) and gradually converted to alcogels at ambient temperature. Subsequently, the wet gels were aged for 2 days in 50 °C water bath, and then washed with ethanol every 12 h and repeated for 2 times. After that, the washed wet gels were dried at ambient pressure in a furnace in three subsequent steps as follows: at 50 °C for 12 h, 80 °C for 2 h and, finally, at 200 °C for 2 h. The heating-rate of this process is 10 °C·min^{-1}. The first and second steps of drying needed more time, which could decrease the probability of crack generation. Suitable temperature in third step was essential for the "spring back effect". If the temperature was 150 °C in the third step, the shrinkage and rigidity of products increase. However, the obtained samples were cracked when the temperature was 250 °C. Therefore, 200 °C was chosen in the third step. In this way, the drying process needed only 16.5 h. The aerogels prepared with varied PDMS/MTES volume ratio (S) of 0, 2.5%, 5%, 6.25%, 7.5%, and 8.75% are noted as S_X (X=0,1,2,3,4,5), respectively.

2.2. Characterizations

The bulk densities of the samples were obtained by their mass to volume ratios. The percentage of porosity (P %) of the aerogel monoliths was calculated using the following equation:

$$P\% = (1 - \frac{\rho_b}{\rho_s}) \times 100 \quad (1)$$

Where ρ_b is the bulk density and ρ_s is the skeletal density of the aerogels which was measured using helium pycnometry. The morphological observation was conducted on a scanning electron microscopy (SEM, Zeiss Supra 55). Solid ^{29}Si and ^{13}C NMR spectra were obtained on a Bruker Avance-300 spectrometer with a 4 mm solids probe using cross-polarization and magic angle spinning at 5 kHz. The solid ^{13}C spectra were externally referenced to the carbonyl peak of glycine (176.1 ppm relative to tetramethylsilane, TMS), and the solid ^{29}Si spectra were referenced to the silicon peak of the sodium salt of 3-trimethylsilylpropionic acid (0 ppm). A Fourier transform infrared spectroscopy (FTIR, Nicolet 8700) was employed to study the chemical bonds of the aerogels. Contact angle (^{O}) measurements were performed using a contact angle meter (Kruss, DSA30) to quantify the degree of hydrophobicity of the aerogels. Nitrogen sorption isotherms were measured with ASAP2020 (Micromeritics, USA), the sample was degassed at 150 °C for 12 h. The specific surface area and pore size distribution were calculated by the Brunauer-Emmett-Teller (BET) method and Barrett-Joyner-Halenda (BJH) method, respectively. The flexibility of the aerogels was investigated in terms of the Young's modulus (Y). The compression test was conducted on a universal testing machine (Instron, model 1185). For uniaxial compression tests, samples were compressed to 60% of its original size at a rate

of 5 mm·min^{-1}, and then the applied load was removed at the same rate.

3. Results and discussion

3.1 Synthesis of silica aerogel

In order to synthesize silica aerogels by ambient pressure drying, the PDMS is selected as the co-precursor to improve the flexibility and toughness of silica matrix. The mechanism of hydrolysis and condensation of silica particles ant the co-polycondensation by the co-precursor can been explained by the following chemical reactions:

Scheme 1. The hydrolysis reaction of MTES.

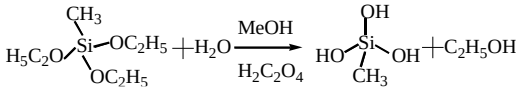

Scheme 2. The condensation of hydrolyzed MTES.

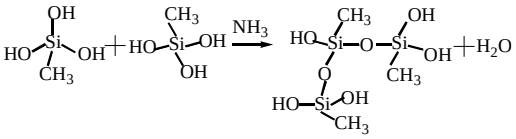

Scheme 3. Co-polycondensation between PDMS and oligomers:

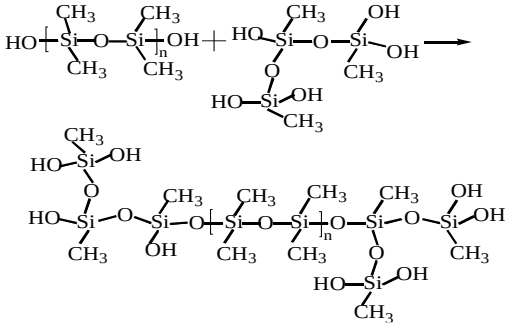

The co-polycondensation reaction proceeds and the silica secondary particles are cross-linked with PDMS according to the reactions of **Scheme 2 and Scheme 3**. As a consequence, the PDMS chain are grafted onto the surface of the silica network, as show in **Fig. 1**.

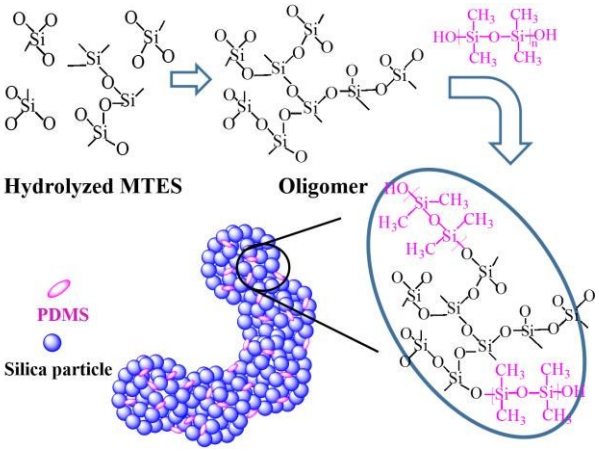

Fig. 1 Reaction scheme of the sol-gel process for MTES-PDMS derived silica aerogel.

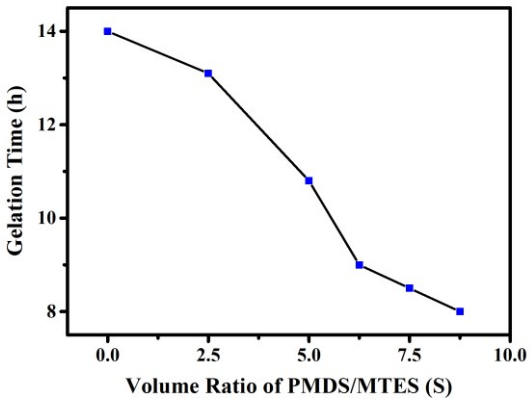

Fig. 2 The variation of gelation time with varied PDMS/MTES volume ratio (S).

Fig. 2 provides the variation of gelation time with varied PMDS/MTES volume ratio (S). The gel time (t_{gel}) is the interval between addition of the ammonia water and the point at which the sols no longer flow when the reaction containers are tilted. The gelation time decreases from 14 h to 8 h with an increase of PDMS/MTES volume ratio (S) from 0 to 8.75%. The decrease of gelation time can be attributed to the fact that the sol particles are easier to separate out from solution because of the winding of PDMS chain with more PDMS contents.

3.2 Solid State $^{13}C/^{29}Si$ NMR and FTIR analysis of the silica aerogels

As show in **Fig. 3a**, the ^{13}C Solid State NMR (SSNMR) from S_0 and S_5 both contains two every weak peaks at 57.7 ppm and 18.5 ppm, which can be assigned to ethoxy groups attached to Si due to incomplete hydrolysis of MTES.[34] According to this fact, it is concluded that only small portion of ethoxy groups is unhydrolyzed. The as-prepared samples were characterized by

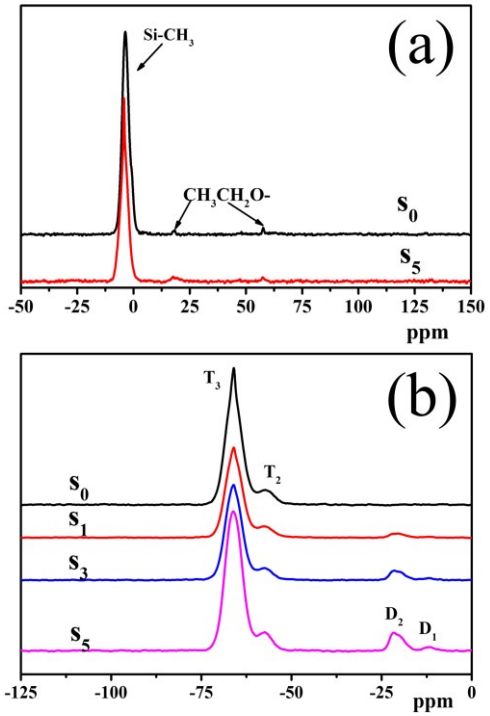

Fig. 3 Solid State ^{13}C NMR spectra (b) of aerogel S_0 and S_5; Solid-state ^{29}Si NMR (b) of aerogel S_0, S_1, S_3 and S_5.

Journal Name

ARTICLE

Table 1 Physical properties of MTES based silica aerogels as a function of the PDMS/MTES volume ratio (S)

Sample	Density ($g \cdot cm^{-3}$)	Linear shrinkage [a] (%)	Porosity (%)	Contact Angle (°)	SA BET ($m^2\ g^{-1}$)	Pore Volume ($mL\ g^{-1}$)	Young's modulus (MPa)
S_0	0.173	-	90. 9	108.3	578.2	2.89	-[b]
S_1	0.124	29.7	93.4	119.5	458.3	1.56	-[b]
S_2	0.098	28.8	94.8	126.8	401.9	0.91	0.136
S_3	0.071	12.8	96.2	133.3	340.8	0.73	0.075
S_4	0.065	11.5	96.6	140.6	325.0	0.63	0.041
S_5	0.064	10.0	96.6	150.8	315.2	0.61	0.030

[a] Linear shrinkage is obtained in the axial direction; [b] Cylindrical samples of S_0 and S_1 can not be prepared.

^{29}Si Solid State NMR (SSNMR) to determine the fraction of PDMS included in the final aerogel specimens. As shown in **Fig. 3b**, the ^{29}Si NMR spectrum from S_0 shows the resonances in the silica region of the spectrum with peaks at -57 ppm (T_2) and -65 ppm (T_3).[12, 35] These peaks arise from the Si sites with the structures of $CH_3Si(-O)_2(-OH)_1$ and $CH_3Si(-O)_3$, respectively. The smaller population of T_2 sites relative to T_3 results from a small number of hydroxyl groups present. The ^{29}Si NMR spectrum from S_5 shows four peaks: T_2, T_3, D_1 (-12 ppm) and D_2 (-22 ppm). The peaks of D_1 and D_2 arise from the the Si sites with the structures of $(CH_3)_2Si(-O)_1(-OH)_1$ and $(CH_3)_2Si(-O)_2$ form PDMS, respectively[32, 36, 37]. Comparison of the peak intensities of Si atom arising from $CH_3Si\equiv$ and $(CH_3)_2Si=$ and the collection of PDMS in wash liquor by completely removing the solvent indicates that nearly all PDMS has been incorporated in the matrix.

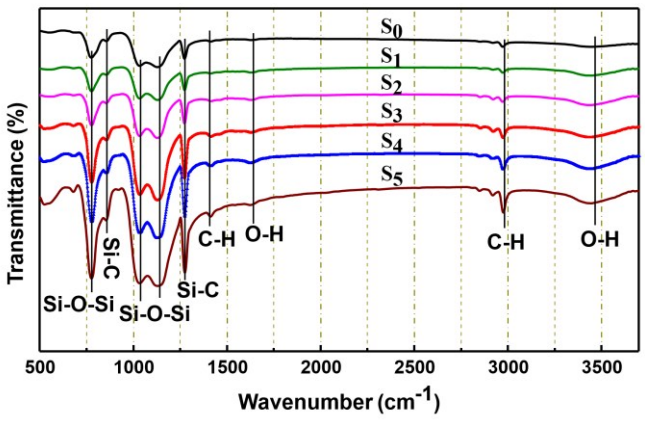

Fig. 4 FTIR spectra of silica aerogel samples prepared with varied S values.

Fig. 4 provides the FTIR spectra of silica aerogels prepared with varied PDMS/MTES volume ratio (S) from 0 to 8.75%. The main bonds of the silica aerogels are Si-O-Si, which appeared at 776 cm^{-1} and between 1033 and 1123 cm^{-1}.[33] The peaks at ca. 1274 and 853 cm^{-1} corresponds to Si-C bonds. The C-H bonds from–CH_3 groups result in the peak at ca.2970 cm^{-1} and 1400 cm^{-1}.[38, 39] It was noticed that a very weak peak appearing at ~2910 cm^{-1}, which are expected to correspond to residual non-hydrolyzed methoxysilane groups ($-OC_2H_5$) or exchange solvent (ethanol) after dying.[40] As shown in **Fig. 4**, the intensity of absorption band of Si–O–Si, Si–C, and C-H groups all show a rising trend with the increase of S value from 0 to 8.75%. The increase of Si–O–Si groups indicates the strength of silica networks are improved with more PDMS chain cross-linked in the underlying silica structure. The increase of Si-C and C-H groups can be attributed to the incorporation of PDMS into matrix of MTES-based silica aerogel, due to the presence of numerous organic methyl in PDMS, imparting higher hydrophobicity to products. The contact angle of samples are listed in **Table 1**. The hydrophobicity of samples increase with increasing PDMS fraction. The sample S_5 exhibits the maximal contact angle (150.8°). These results are in good agreement with previous discussions about formation of PDMS reinforced alcogels.

3.3 Microstructure and textural properties of the silica aerogels

The flexibility and other physical properties of the silica aerogels depend greatly upon the amount of organic groups in the silica network. In the experiment, the amount of organic groups was tailored by varying the PDMS/MTES volume ratio (S) from 0 to 8.75%. **Fig. 5** shows the photographs of silica aerogels prepared with varied volume ratios of PDMS: MTES (S): 0, 2.5%, 5%, 6.25%, 7.5%, and 8.75%, respectively. The physical properties of the flexible silica aerogels prepared with varied PDMS/MTES volume ratio (S) from 0 to 8.75% are listed

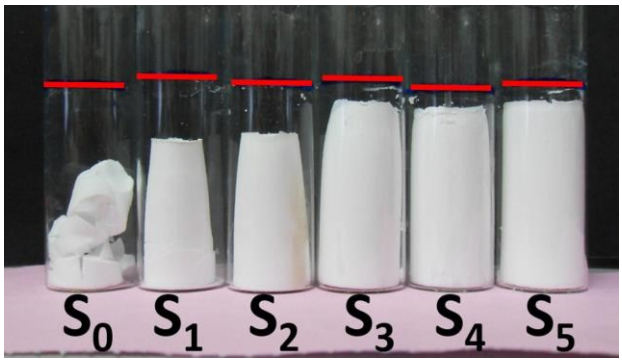

Fig. 5 Photographs of silica aerogel: S_0, S_1, S_2, S_3, S_4, and S_5. The red line on every ampoule tubing represents their volume of wet gel, respectively.

in **Table 1**. Without PDMS (S=0) addition in the starting composition, the aerogel S_0 is a cracked monolith with density of 0.173 g·cm^{-3}. This illustrates that the network of aerogel S_0 is agglomerated and cracked due to the high capillary pressure generated during the ambient pressure drying. If the S is increased, both the linear shrinkage and density of sample obviously decline. As the fraction of PDMS was increased from 2.5% to 8.75%, the linear shrinkage and density of sample can decrease from 29.7 % and 0.124 g·cm^{-3} to 10 % and 0.064 g·cm^{-3}, respectively. The aerogel S_5 is complete cylinder. This indicates that, with the increase of PDMS, not only the connection of adjacent secondary particulates were reinforced, but also the hydrophobicity of silica network increased, resulting in a flexible three-dimensional matrix, so that the gels spring back to near its original volume of wet gel, when evaporation is completed. No monolithic gelation occurred in S>8.75%, because the PDMS modified sol particles are coarsened with more PDMS and only precipitates are obtained due to the flocculation.

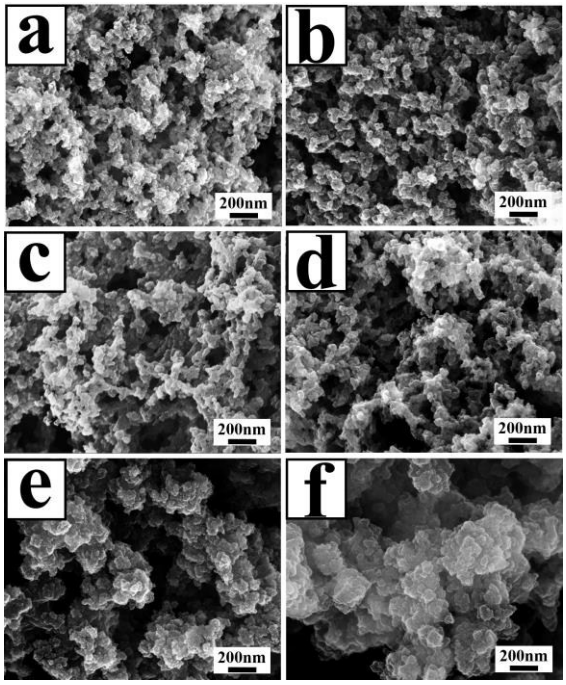

Fig. 6 SEM images of silica aerogels: a) S_0, b) S_1, c) S_2, d) S_3, e) S_4 and f) S_5.

Fig. 6 shows the SEM images of the samples prepared with varied PDMS contents. The S_0 shown in **Fig. 6a** exhibits a dense network structure with smaller particle sizes. With the increase of PDMS contents in the initial sols, the particles are coarsened and a more open pore structure is formed (**Fig. 6b-6f**). In the S_5, the particles look as they have coalesced, giving the appearance of thicker framework with larger porestructure (**Fig. 6f**). This can be attributed to the fact that the adjacent secondary particles are linked with more PDMS, which strengthen the solid skeleton of silica gel to withstand capillary pressure. In addition, the hydrophobic Si-CH_3 groups of PDMS impart more hydrophobic and higher flexible properties to the SiO_2 backbone, which can spring back to its original gel structure after ambient pressure drying.

3.4 Surface Area and pore structure of Silica aerogels

Fig. 7a shows nitrogen adsorption/desorption isotherms of the aerogels S_0, S_1, S_2, S_3, S_4 and S_5, respectively. All samples exhibit hysteresis at relatively high P/Po, which can be classified as Type IV according to the IUPAC nomenclature. The presence of hysteresis loop, caused by the capillary condensation in the mesopore (2-50 nm), suggest the resulting aerogels are mesoporous materials[41]. As shown in **Fig. 7b**, the most probable pore size of all samples mainly centered at ~2 nm and ~50 nm. It is clear that the mesoporous structure decreases with increasing the PDMS contents. The surface

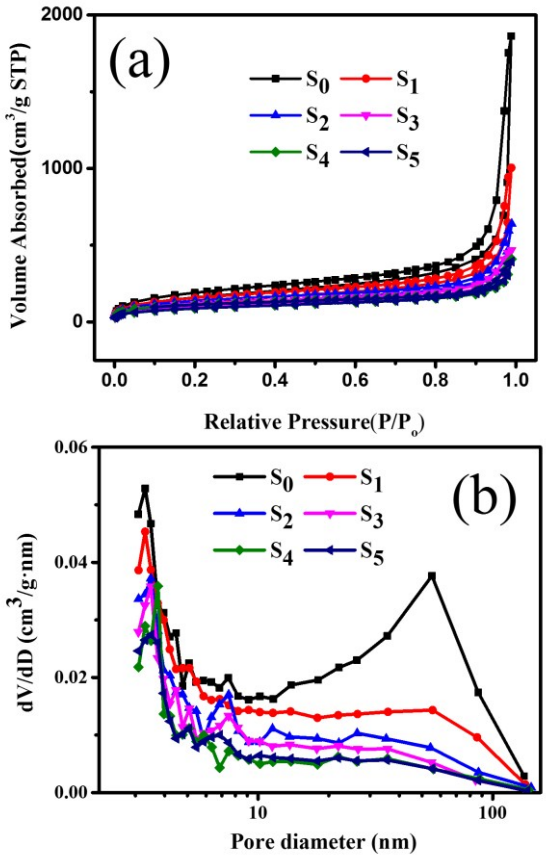

Fig. 7 Nitrogen adsorption-desorption isotherms (a) and the BJH pore size distributions (b) for silica aerogels: S_0, S_1, S_2, S_3, S_4 and S_5, respectively.

area and pore volume average pore diameter for the silica aerogels are summary in **Table 1**. Both the surface area and pore volume show a decline with increasing the amount of PDMS. The sample S_0 prepared with no PDMS exhibits the maximum specific surface area (578.2 $m^2 \cdot g^{-1}$) and pore volume (2.89 $ml \cdot g^{-1}$) among all the as-prepared aerogels. Presumably the cross-linking between silica secondary particles and PDMS blocks the small pores interior to the secondary particles from nitrogen sorption, which results in the decrease of surface area and pore volume. It is noted that the decrease of pore volume is in conflict with the porosity calculated by equation 1. This can be attributed to that a large number of pore in particular macropore is not measured by nitrogen adsorption/desorption method. This paradox about the pore volume and porosity indicates that macropore structure of samples increase with more PDMS. This also can be supported by the SEM date discussed earlier.

3.5 Mechanical properties of Silica aerogels

The uniaxial compressive stress-stain curves of samples with varied PDMS contents are provided in **Fig. 8**. As shown, the samples with larger S tend to need smaller stress in order to get the same strain. Moreover, sample S_2 is fractured when the strain is 55%. Young's modulus of the aerogels exhibit an evidently decline from 0.136 to 0.030 MPa with the increase of S from 5 % to 8.75 %, as listed in **Table 1**, which supports the description of the flexibility tailored by different S value of PDMS. For S_5, up to 70% compressive strain is recoverable. Both obtained Young's modulus and recoverable strain are comparable with the reported values of MTMS-based aerogels (0.3 MPa and 60%) [37] and MTMS-GPTMS based aerogel (0.34 MPa and 70%) [20] via supercritical drying. The values of Young's modulus is lower than that products derived from Vinyltriethoxysilane and 2,2`-(ethylenedioxy)dieth-anethiol (0.11 MPa) [38] by ambient pressure drying. The mechanical results imply that high flexible MTES-PDMS based silica aerogels avoid the costly and hazardous supercritical drying, making it a promising silica aerogel material for larger scale commercial applications.

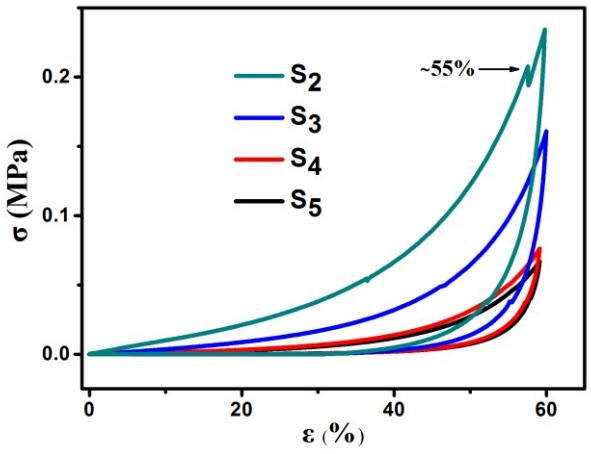

Fig. 8 Stress-strain curves obtained by uniaxial compression on aerogels S_2, S_3, S_4 and S_5.

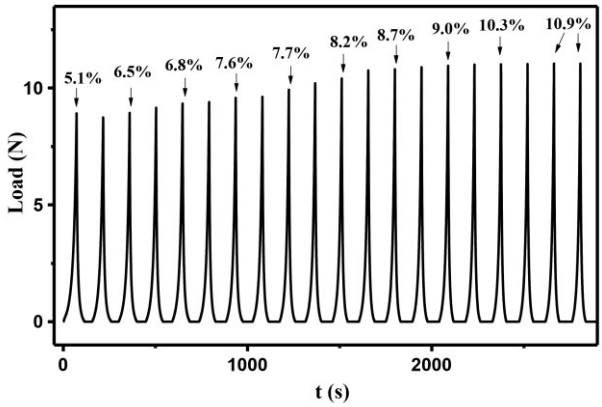

Fig. 9 Load-time circular curves of aerogel S_5. The values on the Load-time peaks are unrecovered strains.

To assess its elastic properties, sample S_5 was compressed to 60% of its original height for 20 consecutive cycles (Movie M1). The Load-time curves for 20 compression cycles of samples S_5 and the unrecovered strains corresponded to compression test are shown in **Fig. 9**. The shapes of these Load-time peaks are almost same as each other. Moreover, the unrecovered strains calculated immediately and 12 h after the compression to 60% strain for twenty times are 10.9% and 3.1%, respectively. The unrecovered strain (%) is calculated as the percentage of initial length that did not recover. These results indicate the PDMS-reinforced silica aerogels have perfect compressible and recoverable property. Using PDMS as an elastic reinforcement to originally enlarge the connection point between silica secondary particles is analogous to graft with methyl groups, giving toughness and flexibility to the network. The samples prepared with more PDMS undergo less shrinkage and have more open pore structures which will offer more free space for the deformation of the skeleton of silica aerogel. Therefore, with an increase of PDMS, the elastic recovery of PDMS reinforced silica aerogel is improved because this increases the flexibility and toughness of the silica networks.

4. Conclusions

The highly flexible, hydrophobic and low-density methyltriethoxysilane-polydimethylsiloxane based aerogels with varied polydimethylsiloxane contents had been prepared via ambient pressure drying. It is proved that the polydimethylsiloxane is an ideal elastic reinforcement for preparing less volume shrinkage at ambient pressure with a simplified solvent evaporation. Results show that both bulk density and Young's modulus decrease with an increase of the polydimethylsiloxane/methyltriethoxysilane volume ratio (S). The microstructure is also easily changed by varying the value of S. The silica aerogel samples prepared at S=8.75% exhibit low bulk density (0.064 $g \cdot cm^{-3}$), high flexibility (0.030 MPa) and hydrophobicity (150.8°). Its maximal recoverable compressive strain is 70%. The unrecovered strains calculated immediately and 12 h after the compression to 60% strain for twenty times

are 10.9% and 3.1%, respectively. Because of the soft and elastic porous structures, these aerogels can enlarge the selection of silica aerogel-materials for special applications.

Acknowledgements

This work was supported by the National Natural Science Foundation of China (51202009 and 51272016), New Teachers' Fund for Doctor Stations, Ministry of Education of China (20120010120004), and Foundation of Excellent Doctoral Dissertation of Beijing City (YB20121001001).

References

1 A. Katti, N. Shimpi, S. Roy, H. Lu, E. F. Fabrizio, A. Dass, L. A. Capadona and N. Leventis, *Chem. Mater.*, 2006, **18**, 285-296.
2 Y. Duan, S. C. Jana, B. Lama and M. P. Espe, *Langmuir*, 2013, **29**, 6156-6165.
3 U. F. Ilhan, E. F. Fabrizio, L. McCorkle, D. A. Scheiman, A. Dass, A. Palczer, M. B. Meador, J. C. Johnston and N. Leventis, *J. Mater. Chem.*, 2006, **16**, 3046-3054.
4 K. I. Jensen, J. M. Schultz and F. H. Kristiansen, *J. Non-Cryst. Solids*, 2004, **350**, 351-357.
5 J. Wen and G. L. Wilkes, *Chem. Mater.*, 1996, **8**, 1667-1681.
6 H. Maleki, L. Durães and A. Portugal, *J. Non-Cryst. Solids*, 2014, **385**, 55-74.
7 Y. Duan, S. C. Jana, A. M. Reinsel, B. Lama and M. P. Espe, *Langmuir*, 2012, **28**, 15362-15371.
8 M. Barczak, P. Borowski and A. Dąbrowski, *Colloid Surf. A-Physicochem. Eng. Asp.*, 2009, **347**, 114-120.
9 S. L. Vivod, M. A. B. Meador, B. N. Nguyen and R. Perry, *Polym. Prepr.*, 2009, **50**, 119-120.
10 M. A. B. Meador, A. S. Weber, A. Hindi, M. Naumenko, L. McCorkle, D. Quade, S. L. Vivod, G. L. Gould, S. White and K. Deshpande, *ACS Appl. Mater. Interface*, 2009, **1**, 894-906.
11 11. B. N. Nguyen, M. A. B. Meador, M. E. Tousley, B. Shonkwiler, L. McCorkle, D. A. Scheiman and A. Palczer, *ACS Appl. Mater. Interface*, 2009, **1**, 621-630.
12 H. Guo, B. N. Nguyen, L. S. McCorkle, B. Shonkwiler and M. A. B. Meador, *J. Mater. Chem.*, 2009, **19**, 9054-9062.
13 J. P. Randall, M. A. B. Meador and S. C. Jana, *ACS Appl. Mater. Interface*, 2011, **3**, 613-626.
14 J. C. Williams, M. A. B. Meador, L. McCorkle, C. Mueller and N. Wilmoth, *Chem. Mater.*, 2014, **26**, 4163-4171.
15 H. Guo, M. A. B. Meador, L. McCorkle, D. J. Quade, J. Guo, B. Hamilton, M. Cakmak and G. Sprowl, *ACS Appl. Mater. Interface*, 2011, **3**, 546-552.
16 Y. Ma, M. Kanezashi and T. Tsuru, *J. Sol-Gel Sci. Technol.*, 2010, **53**, 93-99.
17 N. D. Hegde and A. V. Rao, *J. Mater. Sci.*, 2007, **42**, 6965-6971.
18 D. Y. Nadargi and A. V. Rao, *J. Alloys Compd.*, 2009, **467**, 397-404.
19 D. Y. Nadargi, S. S. Latthe, H. Hirashima and A. V. Rao, *Microporous Mesoporous Mater.*, 2009, **117**, 617-626.
20 20. P. R. Aravind, P. Niemeyer and L. Ratke, *Microporous Mesoporous Mater.*, 2013, **181**, 111-115.
21 G. Carlson, D. Lewis, K. McKinley, J. Richardson and T. Tillotson, *J. Non-Cryst. Solids*, 1995, **186**, 372-379.
22 J. Fricke and A. Emmerlin*g, J. Fricke and A. Emmerling, in Chemistry, Spectroscopy and Applications of Sol-Gel Glasses, Springer, 1992, pp. 37-87.*
23 H. Schäfer, S. Brandt, B. Milow, S. Ichilmann, M. Steinhart and L. Ratke, *Chem. Asian J.*, 2013, **8**, 2211-2219.
24 H. Schäfer, B. Milow and L. Ratke, *RSC Adv.*, 2013, **3**, 15263-15272.
25 N. Hüsing and U. Schubert, *Angew. Chem. Int. Ed.*, 2007, **37**, 22-45.
26 S. Yun, H. Luo and Y. Gao, *RSC Adv.*, 2014, **4**, 4535-4542.
27 P. B. Sarawade, J.-K. Kim, H.-K. Kim and H.-T. Kim, *Appl. Surf. Sci.*, 2007, **254**, 574-579.
28 A. P. Rao, A. V. Rao and G. Pajonk, *J. Sol-Gel Sci. Technol.*, 2005, **36**, 285-292.
29 G. Hayase, K. Kanamori and K. Nakanishi, *J. Mater. Chem.*, 2011, **21**, 17077-17079.
30 S. D. Bhagat, C.-S. Oh, Y.-H. Kim, Y.-S. Ahn and J.-G. Yeo, *Microporous Mesoporous Mater.*, 2007, **100**, 350-355.
31 P. Aravind and G. Soraru, *J. Porous Mater.*, 2011, **18**, 159-165.
32 L. Li, B. Yalcin, B. N. Nguyen, M. A. B. Meador and M. Cakmak, *ACS Appl. Mater. Interface*, 2009, **1**, 2491-2501.
33 T. M. Tillotson and L. W. Hrubesh, *J. Non-Cryst. Solids*, 1992, **145**, 44-50.
34 S. Yun, H. Luo and Y. Gao, *J. Mater. Chem. A*, 2015, **3**, 3390-3398.
35 B. N. Nguyen, M. A. B. Meador, A. Medoro, V. Arendt, J. Randall, L. McCorkle and B. Shonkwiler, *ACS Appl. Mater. Interface*, 2010, **2**, 1430-1443.
36 V. Litvinov, H. Barthel and J. Weis, *Macromolecules*, 2002, **35**, 4356-4364.
37 F. Schilling, M. Gomez and A. Tonelli, *Macromolecules*, 1991, **24**, 6552-6553.
38 M. Ochoa, L. Durães, A. M. Beja and A. Portugal, *J. Sol-Gel Sci. Technol.*, 2012, **61**, 151-160.
39 R. Al-Oweini and H. El-Rassy, *J. Mol. Struct.*, 2009, **919**, 140-145.
40 B. Orel, R. Ješe, A. Vilčnik and U. L. Štangar, *J. Sol-Gel Sci. Technol.*, 2005, **34**, 251-265.
41 R. Pierotti and J. Rouquerol, *Pure Appl. Chem.*, 1985, **57**, 603-619.